XI International Conference on Computational Plasticity. Fundamentals and Applications
COMPLAS XI
E. Oñate, D.R.J. Owen, D. Peric and B. Suárez (Eds)

A METHOD OF TWO-SCALE CHEMO-THERMAL-MECHANICAL COUPLING FOR CONCRETE

Tao Wu*, İlker Temizer†, Peter Wriggers*

*Institute of Continuum Mechanics
Leibniz Universität Hannover
Appelstraße 11, 30167 Hannover, Germany
e-mail: wu,wriggers@ikm.uni-hannover, www.ikm.uni-hannover.de/

†Department of Mechanical Engineering
Bilkent University
06800 Bilkent Ankara, Turkey
e-mail: temizer@bilkent.edu.tr, www.me.bilkent.edu.tr

Key words: Concrete, Alkali Silica Reaction, Multiscale, Homogenization, Coupling

Abstract. The Alkali Silica Reaction(ASR) is one of the most important reasons to cause damage in cementitious constructions, which can be attributed to the expansion of hydrophilic gel produced in the reaction. In this contribution, the chemical extent is described depending on the temperature and it has influences on damage parameters. Expansions of the gel are assumed to only happen in the micropores of Hardened Cement Paste. Afterwards, the homogenization of damage in the microscale is initialized and the effective damage can be applied in the mesoscale directly. Moreover, parameter identification is implemented to extract the effective inelastic consititutive equation. In all, 3D multiscale chemo-thermo-mechanical coupled model is set up to describe the damage in the concrete due to ASR.

1 INTRODUCTION

1.1 Concrete

Concrete is the most widely used construction material in the world because of its good strength and durability. However, it is a exceedingly complex material and has specific structures at different length-scales. This issue can yield stress concentrations which cause overall inelastic behavior in the material. In order to improve the reliability of numerical simulations, it is very crucial to extend the investigation to the microstructure. Concrete at the macroscale is assumed to consist of mortar, large aggregates, large pores, and a

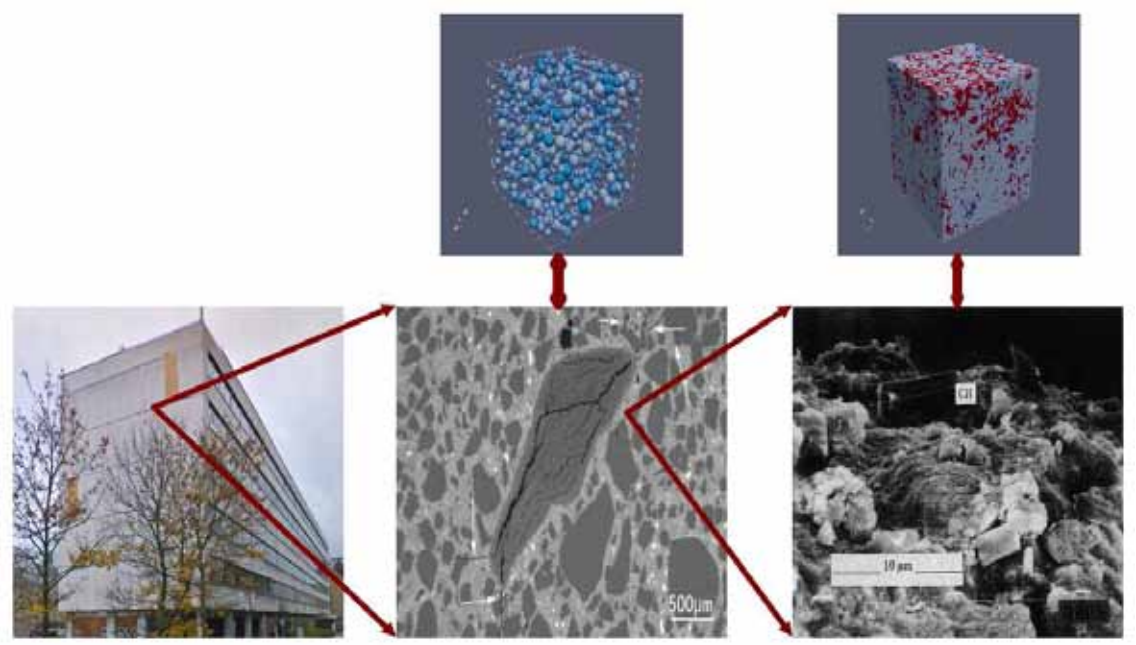

Macroscale *Mesoscale* *Microscale*

Figure 1: Multiscale Representation of the Concrete

cohesive zone between aggregates and mortar. The mortar as the mesoscale contains small aggregates, small pores, hardened cement paste(HCP) and a cohesive zone between small aggregates and HCP. At the microscale, HCP includes hydration products, unhydrated residual clinker and micropores. The whole multiscale representation of concrete is shown in Fig.1.

1.2 Alkali Silica Reaction

1.2.1 Mechanism

The issue of concrete deterioration because of the alkali silica reaction(ASR) has received numerous attentions since 1940[3]. ASR refers to a multistage process, involving non-instantaneous dissolution of silica and instantaneous swelling. The process of dissolution happens at the interface of aggregates and the alkaline solution, where hydroxyl ions attack poorly crystallized silica network. The produced ions from dissolution will combine with positively charged ions to form the gel and then the gel imbibes water and swells. As long as this free expansion space in pore is filled, the gel can exert locally a pressure on the surrounding cement paste which eventually leads the micro-crack and macro-crack of concrete. Many researchers have already agreed the dissolution mechanism of silica as the first stage of the ASR, however, there are debates how the expansion of gel works among researchers until now. The ASR model proposed by Bažant and Steffens[1] assumes that the pressure of water imbibition in the gel can push the gel to permeate the pores in the

cement paste located very near the surface of aggregate particles. Dron and Brivot[2] even go further to assume a through-solution mechanism, where the dissolved silica may diffuse away from the subsequent expansive reactions, may then happen anywhere in the connected pore space of the cement paste. On the other hand Idorn[4] indicates, that the expansive mechanism takes place directly inside the reacting aggregate particles and not in pores or cracks of the cement paste. In addition, Idorn[4] states, that gel penetrating into cracks and pores surrounding the aggregate absorbs calcium ions from the pore liquid. It makes the gel rigid and non-swelling. Up to now, there are no works regarding the alkali silica reaction implemented in the HCP, since some parameters can not be obtained from experiments directly in the microscale, and more importantly, aggregates do not exist in the HCP. The promising character of this contribution is to extend the investigation to the real microscale of concrete. So as to make the microscale model more reasonable, some assumptions have to be set up. Firstly, the expansion of gel is assumed to take place in micropores of the HCP. Secondly, the dissolution process and the expansion process are considered as a one.

1.2.2 Chemical Reaction Kinetics

A first order reaction kinetics is defined here

$$t_c \frac{d\xi}{dt} = 1 - \xi \tag{1}$$

$\xi \in [0, 1]$ is the chemical extent, where 0 indicates no reaction and 1 means the end of reaction. In addition, t_c is the characteristic time depending on the temperature and ξ. Based on experiments from Larive[11], the characteristic time is obtained as

$$t_c = \tau_{ch} \frac{1 + exp[-\tau_{lat}/\tau_{ch}]}{\xi + exp[-\tau_{lat}/\tau_{ch}]} \tag{2}$$

$$\tau_{lat}(T) = \tau_{lat}(\bar{T}) exp[U_{lat}(1/T - 1/\bar{T})]; \qquad \tau_{ch}(T) = \tau_{ch}(\bar{T}) exp[U_{ch}(1/T - 1/\bar{T})] \tag{3}$$

where τ_{lat} and τ_{ch} are the latency time and the expansion time respectively. The values of $U_c = 5400 \pm 500K$, $U_L = 9400 \pm 500K$ are from the literature[5] and afterwards, the evolution of the reaction extent ξ is obtained by integrating the ordinary differential equation (1), see equation (4) and the extent with respect to different temperatures is displayed in Fig.(2).

$$\xi(t) = \frac{1 - exp(-t/\tau_{ch})}{1 + exp(-t/\tau_{ch} + \tau_{lat}/\tau_{ch})} \tag{4}$$

For a genetric temperature history, the accumulated extent can be obtained through the backward euler scheme. In terms of different temperature inputs, the accumulation curve of extent is obtained, see Fig.(4) and Fig.(5).

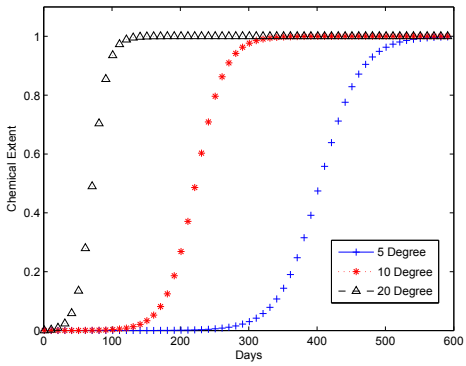

Figure 2: Chemical Extent

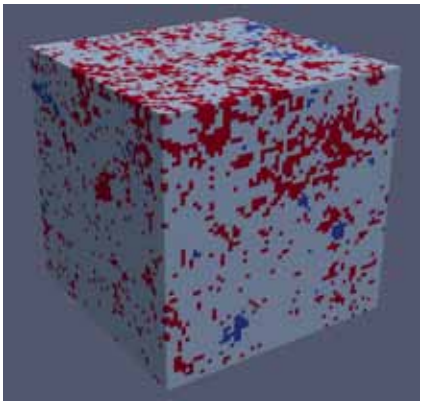

Figure 3: Hardened Cement Paste

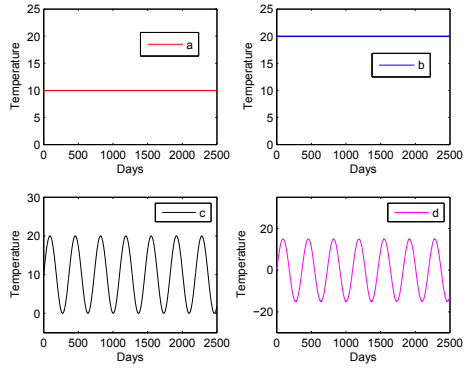

Figure 4: Different Temperatures

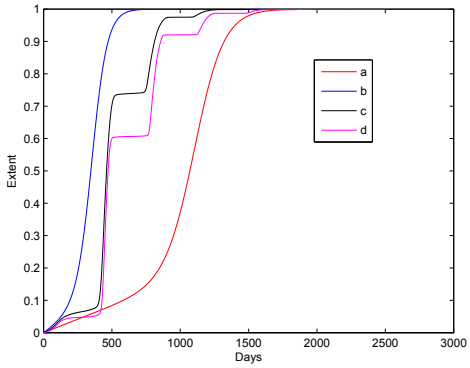

Figure 5: Chemical Extent Accumulation

2 MICROSCALE OF THE CONCRETE

2.1 Representation of the Hardened Cement Paste

The representation of HCP is obtained using three-dimensional micro-CT scans with a spatially resolved distribution of the density. Each voxel is $1\mu m^3$ with only one material identifier. According to the theory of Powers, the fractional volume of hydration products is 83.4% and the fractional volume of micropores is 14.3% when the water-cement ratio is 0.45 and the hydration degree is 0.945. Through the median filter, a final three-dimensional finite-element mesh with three different material identifiers is produced for numerical simulation, which can represent each voxel with a finite-element of hexahedron type, see Fig.(3). Pale parts are hydration products, red part are micropores and blue parts are unhydrated residual clicker.

2.2 Constitutive Equations in the HCP

2.2.1 Hydration Product

2.2.2 Gel

Since the chemistry of gel is similar to the Calcium-Silicate-Hydrate, gel is treated as a incompressible material, with a Possion ratio of 0.49975. Standard displacement elements experience locking for incompressible conditions, hence, Q1P0 is launched to solve this problem. In the case of any deformation, there are deviatoric and volumetric strain components. Deviatoric strains determine the shape change of the body and volumetric strains determine the volume change. The volume change occurs due to a hydostatic pressure. As a result, Q1P0 element determines the shape change from the deviatoric strains and the pressures from the volumetric strain, where the shape function of pressure in FEM is constant. $\sigma = 2\mu\varepsilon^D + P$ and P is the hydrostatic pressure. Herein, $P = \kappa tr\varepsilon - \kappa\beta\xi$, where β is the expansion coefficient and ξ is the chemical extent. The weak forms of the above-mentioned stress formular and the mechanical equilibrium are shown in equation (5) and equation (6).

$$\int_V r(\kappa^{-1}P - (tr\varepsilon - \beta\xi))dV = 0 \tag{5}$$

$$\int_V \varepsilon(\eta) : \sigma(u)dV = \int_V (\varepsilon^D(\eta) + \varepsilon^V(\eta)) : (\sigma^D(u) + P1)dV = \int_V \eta \cdot \rho b dV + \int_\Gamma t \cdot \eta d\Gamma \tag{6}$$

where r and η are the test function for stress and displacement. After plugging equation (5) into equation (6) and the linearization, the tangent matrix and the residual can be obtained.

2.3 Homogenization

Computational homogenization is very critical tool to bridge the microscale and the marcroscale[10]. The resulting effective material behavior can be applied to the mechanical model at the next length-scale through the volume average of representative volume elemnt(RVE). $\langle D \rangle = \frac{1}{V}\int_V D dV$, where $\langle * \rangle$ denotes the volume average of a representative volume element. The size of RVE is very critical for homogenization, which can ensure the statistical representative response under boundary conditions satisfying the HILL's energy criterion. In this contribution, the RVE of 64*64*64 is choosed from Hain[8]. Afterwards the displacement boundary condition of RVE is fixed and just consider the expansion inside of RVE. The effective damage of RVE is increased with the chemical reaction going on for different expansion ratios, see Fig.6. The damage distribution on hardened cement paste is shown in Fig.7.

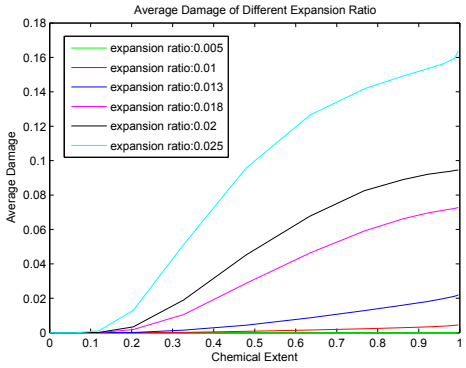

Figure 6: Effective Damage

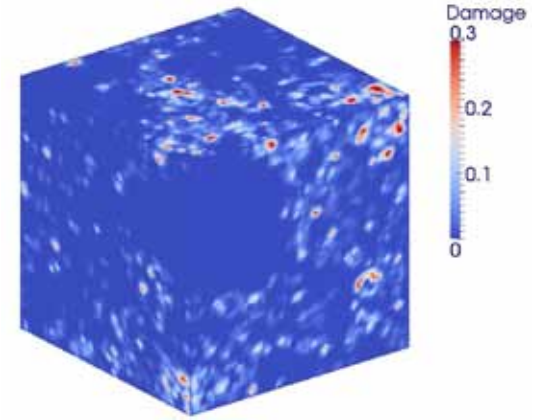

Figure 7: Damage on Hardened Cement Paste

2.4 Statistical Analysis

Because the representative volume element(RVEs) is only a different portion of the HCP, statistical analysis of a sufficient number of different three-dimensional specimens makes numerical simulation of damage more reasonable and accurate. 20 statistical tests are run with the expansion ratio of 0.02, see Fig.(8). The mean value and the standard deviation of homogenized damage-extent correlation are obtained through equation (7). Afterwards, equation (8) is used to approximate $d(\xi)^{med}$ and $d(\xi)^{std}$, which can be directly applied for the computation in the mesoscale. Table (1) demonstrates the approxmation coefficients and referring to the approximation of mean and standard deviation, see Fig.(9) and Fig.(10).

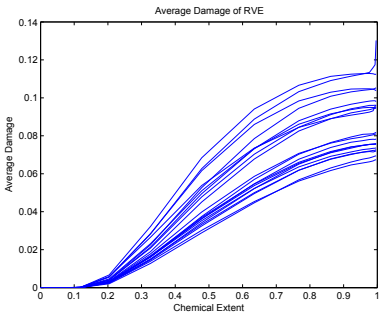

Figure 8: Statistical Tests

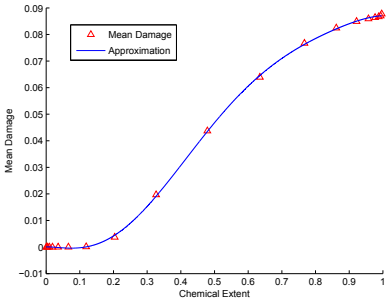

Figure 9: Mean Average

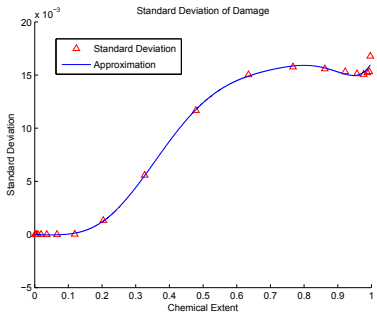

Figure 10: Standard Deviation

$$d(\xi)^{med} := \frac{1}{n}\sum_{i=1}^{n} < d(\xi_i) > \qquad d(\xi)^{std} := \sqrt{\frac{1}{n-1}\sum_{i=1}^{n}[< d(\xi)_i > -d(\xi)^{med}]^2} \tag{7}$$

$$D(\xi)^{med} := \sum_{i=0}^{i\leq 6} c_i^{med}\xi^i \quad and \quad D(\xi)^{std} := \sum_{i=0}^{i\leq 7} c_i^{std}\xi^i \tag{8}$$

i	0	1	2	3	4	5	6	7
c_i^{med}	-1.4539	4.7304	-5.5806	2.6142	-0.2205	-0.0025	0.0001	
c_i^{std}	5.5993	-20.4421	29.2301	-20.2592	6.6718	-0.8509	0.0704	-0.0033

Table 1: Coefficients of Approximation

3 MESOSCALE OF THE CONCRETE

3.1 Take and Place Algorithm

The evaluation of the mesoscale representation of concrete needs the generation of a random aggregate structure where the size and distribution of the coarse aggregates closely resemble real concrete in the statistical sense. This structure is comprised of randomly distributed aggregates particles and mortar matrix filling the space between the particles. This random principle is implemented by taking samples of aggregate particles from a source whose size distribution follows a certain given grading curve, see Fig.11 and Table (2), and then placing the aggregates one by one into the concrete in such a way, which can ensure no overlapping with particles already placed. Grading curve refers to the determination of the particle size distribution for aggregates, usually experssed in terms of cumulative percentage passing through a series of size of sieve openings. In order to place an aggregate particle at a free position within the concrete volume, two obvious conditions need to be satisfied. The whole aggregates must be completely within the boundary of the concrete volume and there must not be any overlapping with previously placed aggregates.

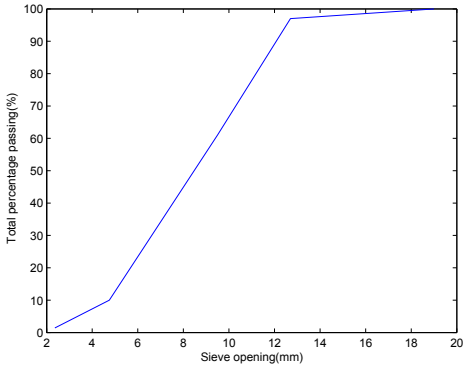

Figure 11: Grading Curve

Size(mm)	Retained(%)	Passing(%)
19.00	0	100
12.70	3	97
9.50	39	61
4.75	90	10
2.36	98.6	1.4

Table 2: Sieve Result

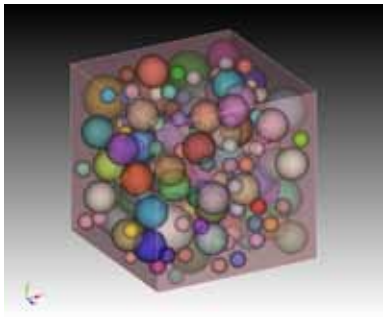

Figure 12: Mesoscale

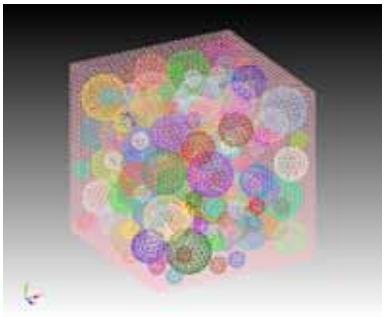

Figure 13: Descritization

3.2 Discretization

Discretization of the generated RVEs consisting of many inclusions is a tedious procedure. There are basically two approaches to mesh the microstructure of the concrete material: an unaligned or an aligned approach. In this contribution, the generated mesostructure model is translated into the commercial software CUBIT which offers the option of automatic mesh generation with tetrahedral elements, then generates the mesh and finally outputs a mesh file for the finite element analysis program (FEAP), which is a nonlinear finite element software.

3.3 Effective Inelastic Constitutive Equation

In the mesoscale, aggregates are assumed to be purely elastic and cement paste is assumed to be an inelastic damage material. Since finding an effective inelastic constitutive equation by homogenization is still an unsolved problem, an inelastic effective constitutive equation with the unknown material parameters must be defined through parameter identification. In terms of the cement paste, a visco-plastic model of PERZYNA-type combined with an isotropic damage model is choosen. Considering the definition of elas-

tic energy rate yields

$$D : 0 \leqslant \sigma : \dot{\varepsilon}^{pl} + Y\dot{D}^{u} \tag{9}$$

a constrained optimization problem combined with the Penalty-Lagrange approach can yield an unconstrained optimization problem.

$$P = -\sigma : \dot{\varepsilon}^{pl} - Y\dot{D}^{u} + \frac{1}{\eta}\phi(f) + \dot{\chi}S^{u} \rightarrow stat \tag{10}$$

where the variable $\frac{1}{\eta}$ refers to the penalty-parameter, $\phi(f)$ denotes the penalty function, and χ is the LAGRANGE multiplier. A partial differentiation of P with respct to the elastic energy rate Y yields the evolution equation of damage.

$$\dot{D} = \xi\frac{\partial S(\varepsilon^{eq})}{\partial \varepsilon^{eq}} \tag{11}$$

where $S(\varepsilon)$ is the damage surface determining whether damage increases or not. It depends on the equivalent strain ε^{eq}.

$$S(\varepsilon) := 1 - exp\left[-\left(\frac{\varepsilon^{eq} - a}{b}\right)^{c}\right] - D \leqslant 0 \tag{12}$$

The damage surface is defined by an exponential law and depends on the elastic energy ε^{eq}, in addition, the parameters $a, b, and\ c$ are the material properties of the assumed model. The partial differentiation of P with respect to the σ yields the plastic strain evolution.

$$\dot{\varepsilon}^{pl}_{n+1} = \frac{1}{\eta}\phi^{+}\frac{\partial f}{\partial \sigma} \tag{13}$$

where ϕ^{+} denotes the derivative of the penalty function $\phi(f)$ and the penalty function itself is defined the $(k+1)th$ power of the yield surface f. The material property k is assumed to take the value $k = 1$ in order to enable a nonlinear viscous behavior.

$$\phi(f) = \begin{cases} 0 & ;\text{f}\leqslant 0 \\ \frac{1}{k+1}f^{k+1} & ;\text{f}>0 \end{cases} \tag{14}$$

The abovementioned penalty function ensures that the constraint f is satisfied apprximately which is typical for visco-plastic materials. The yield surface f is assmed to be of VON-MISES-type

$$f := \alpha tr\sigma + \|dev\sigma\| - \sqrt{\frac{2}{3}}k_f \leqslant 0, \tag{15}$$

where $dev\sigma$ denotes the deviatoric part of the stress tensor, $tr\sigma$ is the trace of the stress tensor, and k_f is the material property of the model. Eventually, the equation (13) can be solved with the radial return mapping procedure based on the implicit Euler scheme.

3.4 Parameter Identification

Because the parameters in the abovementioned equation can not be obtained from experiments, parameter identification is formulated as an optimization problem, where a least-squares functional is minimized for providing the best agreement between experimental data and numerical data. The objective function is generated and then the material properties are calculated on the basis of minimization of the objective function. The objective function $A(\kappa)$ is defined as a least-square sum between the experiment[9] and the numerical result: $A(\kappa) := \sum(\langle\sigma(\kappa)\rangle_i - \sigma_i^{exp})^2 \rightarrow min$. Herein, the combination of Genetic algorithm and Levenberg-Marquardt algorithm is used. The genetic algorithm is used for pre-optimization and then the optimization will switch to the Levenberg-Marquardt method, once the object function is smaller than a certain value. It is a efficient and robust algorithm. The optimization results and resulting parameters are shown in Fig.14 and Table 3.

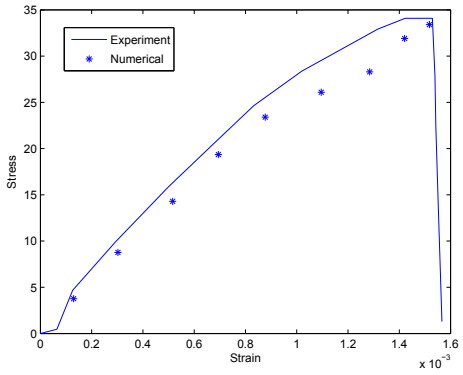

Figure 14: Optimization Result

	κ_0	κ_{min}	κ_{max}	κ^*
k_f	21	20	70	42
η	2725	1000	15000	3525
Δt	0.0015	0.001	0.2	0.0355
b	100	100	5000	4241
a	100	100	2000	718

Table 3: Optimization Parameters

4 THERMAL FIELD

The instationary thermal balance equation states that changing of the temperature is equal to the heat flux q through the surface

$$\int_V \rho c\dot{\theta} dV = -\int_\Gamma q d\Gamma \tag{16}$$

where c denotes the capacity of heat and the heat flux $q = -kgrad\theta$.

5 COUPLING

After imposing the constant temperature on top of the concrete, the heat flux continues to diffuse and then the chemical extent on each gauss point of finite elements could be updated through the backward euler scheme depending on the tempeature. Meanwhile, the chemcial extent can trigger damage which is comprised of the damage due to the alkali silica reaction and the mechanical loading. The evolution of the chemical extent and the

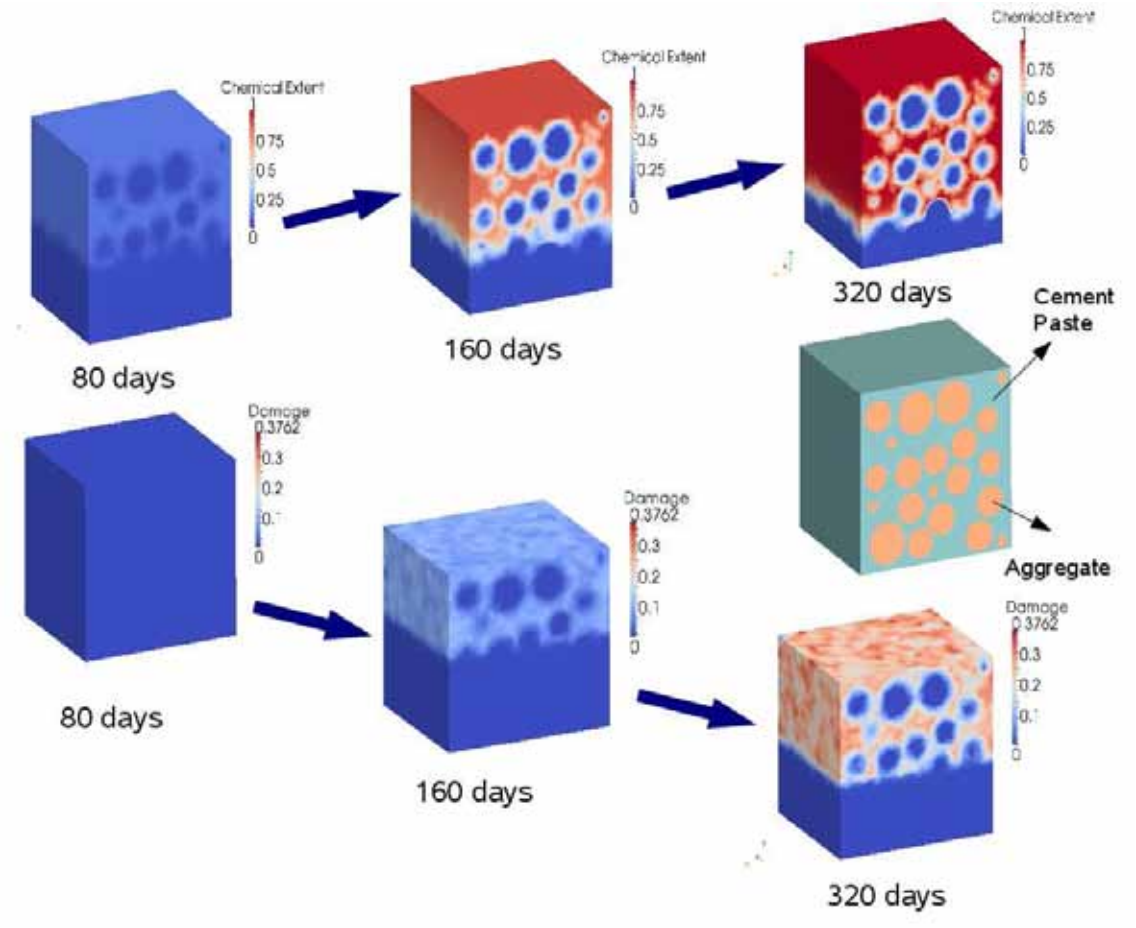

Figure 15: Coupling Result

damage with respect to time is demonstrated in Fig.15. Because aggregates are assumed to be elastic, the chemical extent and the damage do not exist in aggregates.

6 CONCLUSIONS

In this contribution, the mechanism of Alkali Silica Reaction and the representation of concrete in the microscale and mesoscale for further numerical computation are introduced. The numerical homogenization approach is set up to bridge the microscale and macroscale. Furthermore, the parameters of the effective consititutive equation are obtained through parameter identification. Eventually 3D multiscale chemo-thermo-mechanical FEM is demonstrated completely to describe damage in the concrete due to the Alkali Silica Reaction. In the future, the humidity will be incorporated and then the coupling based on the staggered method will be implemented. In addition, because the cohesive zone between aggregates and cement paste in the concrete is very week, the interfacial damage should be considered.

7 ACKNOWLEDGMENT

The first author wishes to thank Stefan Löhnert for helpful discussions.

REFERENCES

[1] Bažant, Z.P. and Steffens, A. Mathematical model for kinetics of alkali-silica reaction in concrete. Cement and Concrete Research. (2000) 30:419-428.

[2] Dorn, R. and Brivot, F. Thermodynamic and kinetic approach to the alkali-silica reaction. Part 2: experiment. Cement and Concrete Research. (1993) 23:93-103.

[3] Lemarchand, E., Dormieux, L. and Ulm, F.J. Elements of micromechanics of ASR-induced swelling in concrete structures. Concrete Science and Engineering. (2002) 4:12-22.

[4] Idorn, G.M. A discussion of the paper 'Mathematical model for kinetics of alkali-silica reaction in concrete' by Zdeněk P.Bažant and Alexander Steffen. Cement and Concrete Research. (2001) 31:1109-1110.

[5] Ulm, F.J., Coussy, O., Li, K.F. and Larive, C. Thermo-chemo-mechanics of ASR expansion in concrete structure. Journal of Engineering Mechanics. (2000) 126:233-242.

[6] Comi, C., Fedele, R. and Perego, U. A chemo-thermo-damage model for the analysis of concrete dams affected by alkali-silica reaction. (2009) 41:210-230.

[7] Wriggers, P. and Moftah, S.O, Mesoscale models for concrete: homogenisation and damage behavior. Finite Elements in Analysis and Design. (2006) 42:623-636.

[8] Hain, M. and Wriggers, P. Computational Homogenization of micro-structural Damage due to Frost in Hardened Cement Paste. Finite Elements in Analysis and Design. (2008) 44:233-244

[9] Comby-Peyrot, I., Bernard, F., Bouchard, P.O., Bay, F. and Garcia-Diaz, E. Development and validation of a 3D computational tool to describe concrete behaviour at mesoscale. Application to the alkali-silica reaction. Computational Materials Science. (2006) 46,1163-1177.

[10] Temizer, İ and Zohdi, T.I. A numerical method for homogenization in non-linear elasticity. Computational Mechanics. (2007) 40:281-298.

[11] Larive, C. Apports combinés de l'expérimentation et de la modélisation à la compréhension de l'alcali-réaction et de ses effects mécaniques. Ph.D thesis, Laboratoire Central des Ponts et Chaussées, Paris, (1998).